ITM Web of Conferences **14**, 00006 (2017) DOI: 10.1051/itmconf/20171400006
APMOD 2016

Aerodynamic shape optimization of an airliner elastic wing

Jan Navrátil[1,⋆]

[1] *Brno University of Technology, Faculty of Mechanical Engineering, Czech Republic*

Abstract. Aerodynamic shape optimization of a common airliner elastic wing is presented and compared with optimization of the same wing assuming rigid structure. A gradient-based optimization approach is applied in connection with adjoint method used for calculation of gradients of aerodynamic forces. The initial wing shape is parameterized by Free Form Deformation technique. The aerodynamics of the elastic wing is calculated using the fluid-structure interaction method which couples computational fluid dynamic solver with linear structural solver.

1 Introduction

An aerodynamic shape optimization using high-fidelity flow solvers has been employed for improvement of aircraft aerodynamic design over the last decades. The growing interest in this field was enabled by developments of the Computational Fluid Dynamics (CFD) solvers. CFD solvers became the accepted analysis tools in the aerospace industry reducing the number of tunnel measurements and flight tests during an aircraft development. Due to usual large number of design variables needed for aerodynamic shape design of aircraft, the gradient-based algorithms combined with adjoint solvers are only meaningful methods for practical application. Locality of those algorithms is a drawback if applied in design space where multiple local optima are likely to occur, the wing shape design is probably such a case. This restricts the process to find only a local optimum near an initial starting point. The solution might be the hybrid optimization algorithms combining non-deterministic (gradient-free) and gradient-based approaches.

The practical application of the gradient-based methods has been probably started by introduction of adjoint sensitivity analysis for Navier-Stokes equation by Pironneau in 1973 [1] and later for incompressible Euler equations [2]. The application in transonic flow regime was enabled by adjoint derivation for compressible Euler equation by Jameson in 1988 [3]. Later he extended the adjoint for Navier-Stokes equations [4]. But the stability and reliability was problem for long period of time. Today, there is only few adjoint Navier-Stockes solvers applying linearized turbulence models, others rely on approximation by frozen eddy viscosity.

Obviously, the aircraft design is multi-disciplinary problem. Increased flexibility of aircraft primary structure, as result of modern material application, requirement for lightweight structure and aerodynamically efficient shapes, even emphasizes the multi-disciplinary nature. The wing deformation due to aerodynamic load results, among others effects, in aerodynamic characteristics change. Thus, the performance gain as result of rigid model optimization might be decreased or neglected

⋆e-mail: navratil@fme.vutbr.cz

if applied to real aircraft. The solution might be inclusion of an airframe elasticity to aircraft shape optimization.

In the paper, the aerodynamic shape optimization of a common airliner elastic wing is presented and compared with optimization of the same wing assuming rigid structure. The aim is evaluation of possible benefit and the computational cost of the aerodynamic shape optimization of the elastic wing. A gradient-based optimization approach is applied in connection with adjoint method used for calculation of aerodynamic forces gradients. The coupled fluid-structure numerical solver is employed for estimation of the elastic wing aerodynamic characteristics.

2 Principle of aerodynamic shape optimization

The schematic of the applied aerodynamic shape optimization loop is given in Figure 1. An optimization algorithm directs a decision making in shape design process in order to improve desired aerodynamic characteristics (drag, glide ration, ...) by minimizing relevant objective function. A parameterization method is employed to describe a given geometry by set of parameters creating a design space. Since the parameterization deforms the surface mesh of the geometry, a mesh deformation tool must be incorporated to propagate the shape deformations into a CFD volume mesh. In the next step, the flow field is solved using CFD solver in case of a rigid model optimization, or coupled CFD with Computational Structural Mechanics (CSM) solver in case of an elastic model, providing the values of flow field variables and integral aerodynamic characteristics of the current design.

Gradients of desired variables (drag, lift, moment coefficients) with respect to all surface mesh nodes displacements are calculated on current shape using adjoint of flow equations solver. In the elastic optimization case, the gradients are calculated on current aeroelastically deformed shape. The gradients with respect to design parameters are obtained by multiplication of the surface gradient vector by parameterization Jacobian matrix. The function and gradient values are fed to the optimizer and the loop is repeated until convergence criteria are met.

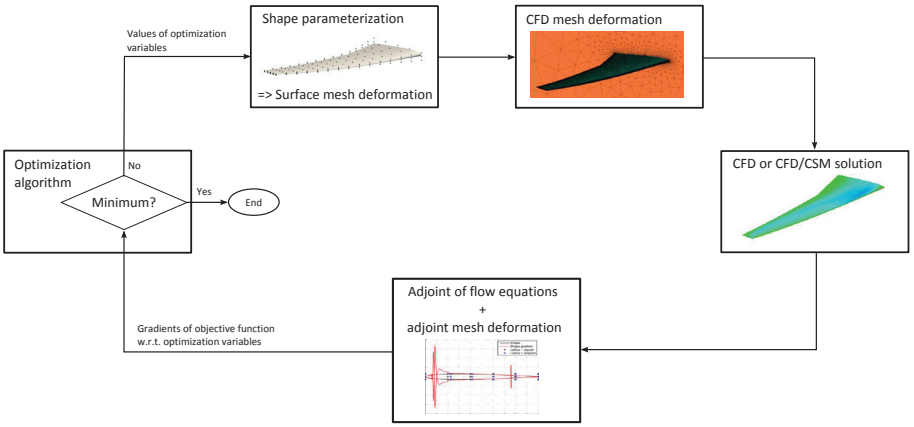

Figure 1. The aerodynamic shape optimization

3 Test cases

3.1 Tools

Flow and adjoint solvers:

The CFD code Edge [5] is used as flow and adjoint of flow equations solver. It is finite volume solver for unstructured grids which can solve 2D and 3D Euler and RANS equations, as well as the adjoint equations of the Euler and RANS (frozen viscosity) equations [6]. The time integration uses the fourth order Runge-Kutta scheme. It employs local-time-stepping, local low-speed preconditioning, multi-grid and dual-time-stepping for steady-state and time-dependent problems. The data structure of the code is edge-based. The solver can parallelize the calculation on a number of processors to solve large flow cases efficiently.

The static aeroelastic solution was obtained by coupling of the CFD Edge with the own simple CSM solver employing the beam finite elements.

Parameterization method:

A Free Form Deformation (FFD) parameterization based on NURBS was employed for a geometry parameterization. This implementation uses RBF coordinates transformation in order to better control deformations and the geometric constraints. The study of numerical properties [7] suggest the highest possible NURBS degree is beneficial from the perspective of the computational cost and the obtained optimization result.

Optimization algorithm

The optimizations were performed by gradient-based optimization algorithm - Sequential Quadratic Programming (SQP) in NLPQLP [8].

Mesh generation and deformation

The initial CFD grid was created in Ansys ICEM CFD. The spring analogy mesh deformation tool was employed to propagate surface shape changes, resulting from the optimization process, into the CFD volume mesh. For large deformations, such as the wing deformation due to the aerodynamic loading, the RBF mesh deformation combined with the spring analogy method was incorporated. The advantage of the RBF based mesh deformation is a capability to handle large deformations, but the surface deformation is not exactly recovered. The error depends on the settings of the mesh deformation solver. Therefore, the inexact surface shape was corrected by the spring analogy mesh deformation, in order to avoid introduction of an error into the optimization process by incorrect mesh deformation.

3.2 Description

The aerodynamic shape optimization test cases, based on cases proposed in [9], concern drag minimization of the transonic wing of the airliner model (so called Common Research Model [10]) at Mach number $M = 0.85$ and altitude $h = 11000m$. The lift coefficient required for steady horizontal flight in such conditions is $C_L = 0.5$. The formulation of the optimization was:

$$\begin{aligned} \text{minimize } F(X) &= C_D \\ \text{subject to } C_L &= 0.5 \\ C_m &\geq -0.1754 \\ V &\geq V^{CRM} \\ t_f &\geq t_f^{CRM} \\ t_r &\geq t_r^{CRM} \\ &\text{fixed trailing edge} \\ &\text{wing planform shape fixed} \end{aligned} \tag{1}$$

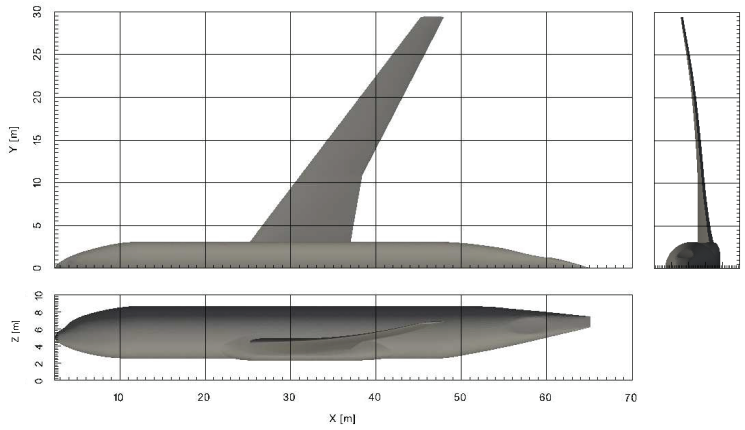

Figure 2. Common Research Model.

The goal is to decrease the drag while the lift remains constant. The geometrical constraint on the internal volume should ensure minimal space for the fuel. Other constraints on the wing thicknesses at front and rear spar positions, t_f and t_r respectively, are meant to guarantee the same minimal structural height thus the minimal structural stiffness is ensured. Therefore, the structural stiffness can remain frozen in the elastic wing optimization case.

The constraints on fixed wing planform shape and fixed trailing edge are not explicitly prescribed, but they are fulfilled by the choice of optimization variables. The Figure 3 shows the FFD lattice fitted on real geometry (in fact, the lattice is orthogonal and the geometry is transformed to fill it, description are in [7]). The blue points in the figure are optimization parameters (totally 216) allowed to move in vertical direction, therefore the airfoils shape together with twist angle are able to change while the planform shape is kept constant. The fixation of trailing edge is achieved by fixed FFD lattice points along the trailing edge, represented by red color in the figure.

Rigid wing optimization:

The initial geometry for the rigid wing optimization cases was the CRM wing as it was given in [10]. The CRM geometry was designed to provide common representative model of an airliner operating

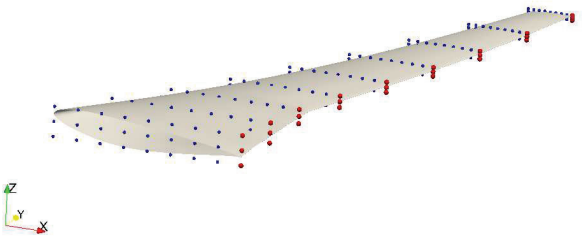

Figure 3. The FFD lattice around CRM wing, blue points are free to move in Z direction, red points are fixed.

Table 1. Aerodynamic characteristics of the initial CRM wing

	Rigid	Aeroelastic
Lift coefficient, C_L	0.5000	0.5000
Drag coefficient, C_D	0.0120	0.0120
Pitch moment coefficient, C_m	−0.1750	−0.1717
Angle of attack, α	0.721	0.816

in transonic conditions for validation of the state-of-the-art CFD solvers. Thus, the geometry of the CRM wing corresponds to flight shape (1-g shape, bended and twisted due to aerodynamic loading) at nominal cruise conditions at Mach $M = 0.85$ and $C_L = 0.5$ at altitude 12 000 m. Therefore, the subject of the optimization is a rigid wing flight shape at its nominal cruise conditions.

Elastic wing optimization:

For the elastic wing optimization, it is desirable to use an undeformed wing geometry as the static aeroelastic analysis determines correct flight shape for given operating condition. Therefore, so called jig shape was designed from the flight shape giving the undeformed wing surface and structural model. The jig shape CFD mesh was created from the mesh of the rigid wing flight shape. Applied structural model is a beam stick finite element model created by 41 beam elements. Each node of the beam element is connected with 2 additional nodes by rigid elements which are beneficial for coupling with aerodynamic surface.

The flow was solved as compressible inviscid. Assuming steady and fully turbulent flow for all designs and the constrained minimum wing wetted area, only lift-induced and wave drag can be minimized. Both flow features can be resolved by Euler flow simulation. Therefore, the optimization using the Euler flow simulation can give reliable and less expensive (in terms of computational effort) estimation of the drag reduction which could be achieved by RANS flow simulations.

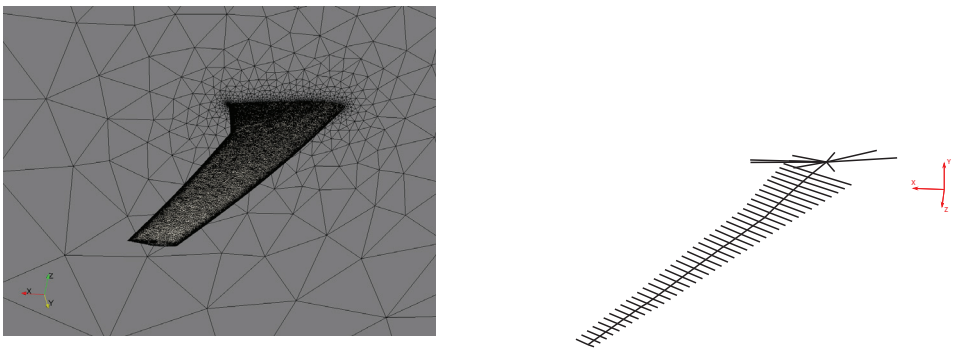

Figure 4. Computational models -the CFD mesh with 933502 nodes (left) and the beam finite element model with 41 beam elements (right).

4 Results

The comparison of both optimization approaches results is presented in Table 2. The constraint imposed on the value of the lift and the pitch moment coefficients was fulfilled, in both cases. The wing internal volume constraint was satisfied in the rigid wing case. In other case the violation was about 0.19%, what might be considered as constraint satisfaction. The optimization objective - the drag coefficient - was reduced by 6.72% and 6.17% in the rigid and elastic wing optimization, respectively. The computational cost, in terms of number of the flow and the adjoint solutions, is nearly twice as high in case of the elastic wing compared to rigid wing case.

The plots in Figure 5 suggest that constraints on the wing thickness were fulfilled in both cases. The thickness at rear spar position remained nearly unchanged in both cases, while the thickness at the front spar was slightly increased near the wing root.

The tuning of the wing shape and the twist angle of the wing sections resulted in redistribution of the lift along wing span. The resultant distribution is closer to ideal elliptical C_Lc distribution, as it is illustrated in Figure 6. Moreover, the lift force resultant was shifted towards wing root what might result in lower bending loading of the wing structure. The same figure shows the wing twist was changed towards higher negative values in both cases.

The Figure 8 presents the pressure coefficient distribution over the upper surface and at chosen wing sections. The plots suggest in both cases the optimization resulted in nearly shock free solution at the nominal cruise condition. The pressure change is more gradual towards the trailing edge of the optimized wing contrary to the baseline wing with steep increase of the pressure due to shock.

Table 2. Comparison of the rigid and elastic wing optimization results

	$C_{D_{opt}}$	$C_{L_{opt}}$	$C_{m_{opt}}$	V_{opt}	Cost[a]	C_D decrease
Baseline	0.0120	0.5000	−0.1750	84.46	–	–
Rigid wing	0.0112	0.5000	−0.1754	84.46	84	6.72%
Elastic wing	0.0113	0.4998	−0.1755	84.28	149	6.1739%

[a] Total cost of optimization in terms of number of flow and adjoint of flow solutions

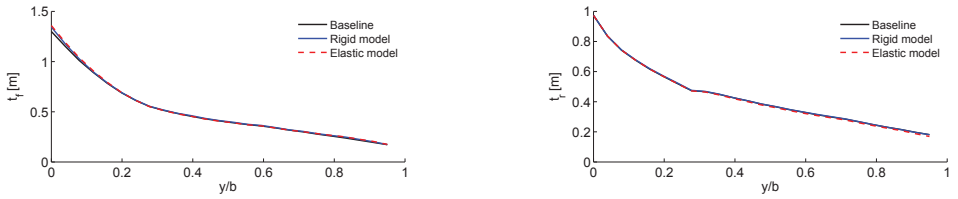

Figure 5. Comparison of the wing thickness, at position of the front (left) and rear (right) wing spar.

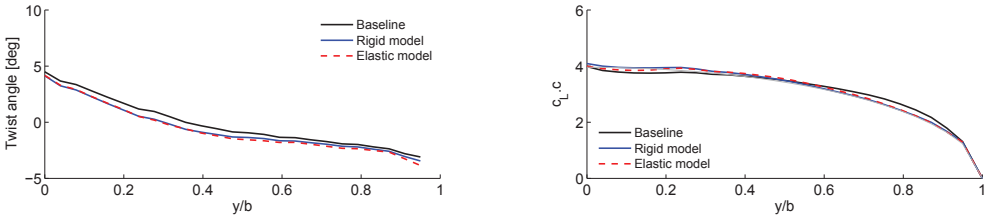

Figure 6. Comparison of span-wise wing twist and lift distributions (grey line shows the elliptical distribution of $C_L c$).

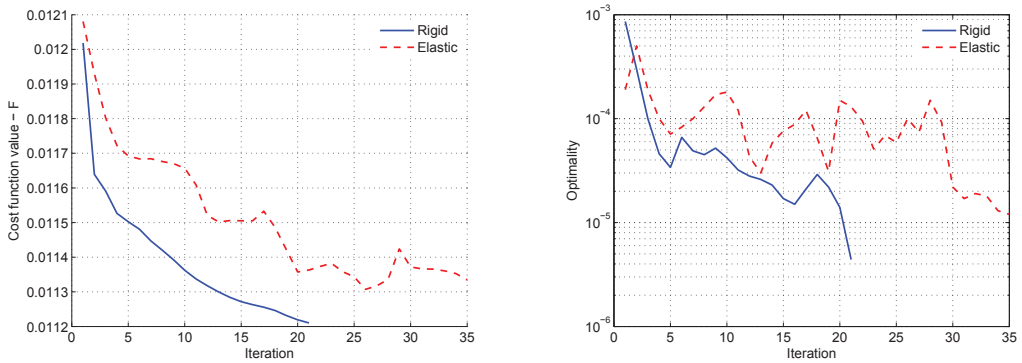

Figure 7. History of the optimization

The optimization history plots shown in Figure 7 suggest the objective function decrease was smooth and the optimization criteria were met after 21 iterations in rigid wing case. The peaks in the plot of the objective function history in case of the elastic wing together with abrupt changes of the optimality imply that there was some source of an error in the optimization chain. The probable source is the neglect of the structural deformation influence on the gradient of the aerodynamic forces and moments. Thus, implementation of the coupled fluid-structure adjoint equation solver is required.

DOI: 10.1051/itmconf/20171400006

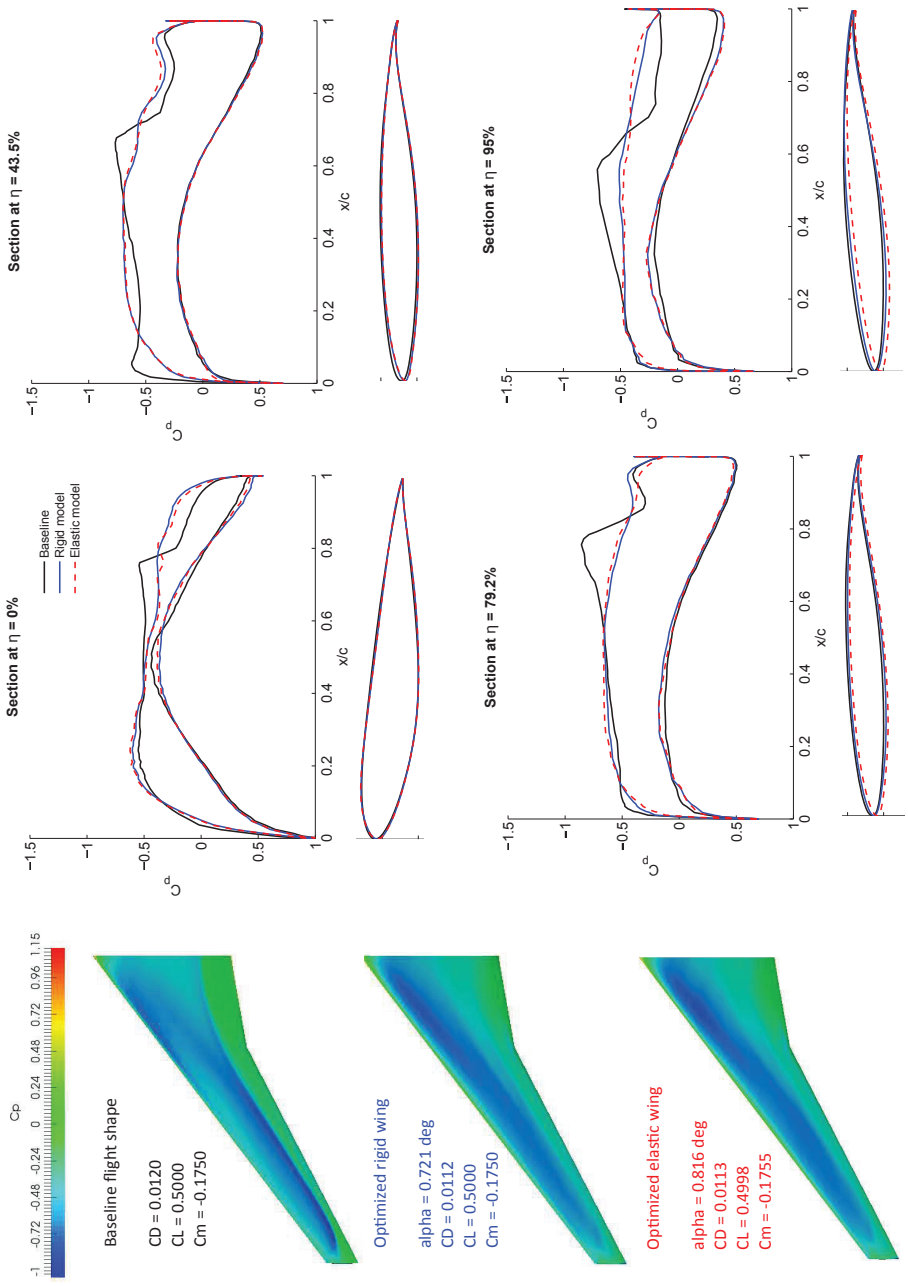

Figure 8. Comparison of surface pressure coefficient distribution - baseline and optimized wings.

5 Conclusion

The paper presents the optimization of the elastic wing compared to the rigid wing optimization. Different initial designs were applied in respective cases for the reasonable comparison. The rigid wing was optimized starting from the flight shape at the design operating conditions. Whereas in case of the elastic wing the initial design was the jig shape which under loading by aerodynamic forces at the design flight conditions deforms to the same flight shape as in rigid case.

The resultant drag reduction is nearly same in both cases, but the computational cost in the elastic wing case is almost twice as high. Moreover, the objective function decrease was not smooth as it might be expected. The several increases of the objective value during the optimization were probably result of inexact gradient calculation. Although the gradients were calculated on the aeroelastic deformed shape, the error in gradient calculation applying pure flow adjoint equation, thus neglecting the influence of the wing structure deformation on the aerodynamic forces gradients, is significant.

Thus, the derivation and implementation of the coupled fluid-structure adjoint equations is necessity for the further work on the elastic wing optimization. The real benefit of this approach is expected in the multi-point optimization considering more operation conditions.

Acknowledgments

Author would like to acknowledge funding from the Ministry of Education, Youth and Sports of the Czech Republic under the National Sustainability Programme I - Project LO1202.

References

[1] O. Pironneau, Journal of Fluid Mechanics **59**, 117 (1973)
[2] O. Pironneau, Journal of Fluid Mechanics **64**, 97 (1974)
[3] A. Jameson, Journal of scientific computing **3**, 233 (1988)
[4] A. Jameson, L. Martinelli, N. Pierce, Theoretical and computational fluid dynamics **10**, 213 (1998)
[5] P. Eliasson, *EDGE, a Navier-Stokes solver for unstructured grids*, in *Proc. to Finite Volumes for Complex Applications III* (ISBN 1 9039 9634 1, 2002), pp. 527–534
[6] O. Amoignon, M. Berggren (2003)
[7] O. Amoignon, J. Hradil, J. Navratil, *A numerical study of adaptive FFD in aerodynamic shape optimization*, in *52nd Aerospace Sciences Meeting* (2014), Vol. 899
[8] K. Schittkowski, *Nlpqlp: A fortran implementation of a sequential quadratic programming algorithm with distributed and non-monotone line search-user's guide* (2006)
[9] L. Osusky, B. H., Z.D. W., Aiaa aerodynamic design optimization discussion group (2013)
[10] J. Vassberg, M. Rivers, R. Wahls, *Development of a Common Research Model for Applied CFD Validation Studies*, in *26th AIAA Applied Aerodynamics Conference* (2008)